

Accepted Manuscript

In silico studies, synthesis and pharmacological evaluation to explore multi-targeted approach for imidazole analogues as potential cholinesterase inhibitors with neuroprotective role for Alzheimer's disease.

Archana S. Gurjar, Mrunali N. Darekar, Keng Yoon Yeong, Luyi Ooi

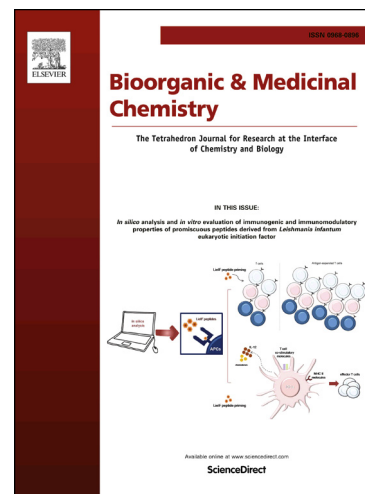
PII: S0968-0896(17)31824-2
DOI: <https://doi.org/10.1016/j.bmc.2018.01.029>
Reference: BMC 14183

To appear in: *Bioorganic & Medicinal Chemistry*

Received Date: 17 September 2017
Revised Date: 27 January 2018
Accepted Date: 31 January 2018

Please cite this article as: Gurjar, A.S., Darekar, M.N., Yeong, K.Y., Ooi, L., *In silico* studies, synthesis and pharmacological evaluation to explore multi-targeted approach for imidazole analogues as potential cholinesterase inhibitors with neuroprotective role for Alzheimer's disease., *Bioorganic & Medicinal Chemistry* (2018), doi: <https://doi.org/10.1016/j.bmc.2018.01.029>

This is a PDF file of an unedited manuscript that has been accepted for publication. As a service to our customers we are providing this early version of the manuscript. The manuscript will undergo copyediting, typesetting, and review of the resulting proof before it is published in its final form. Please note that during the production process errors may be discovered which could affect the content, and all legal disclaimers that apply to the journal pertain.



***In silico* studies, synthesis and pharmacological evaluation to explore multi-targeted approach for imidazole analogues as potential cholinesterase inhibitors with neuroprotective role for Alzheimer's disease.**

Archana S. Gurjar^{a*}, Mrunali N. Darekar^a, Keng Yoon Yeong^b, Luyi Ooi^b

^a *Prin. K. M. Kundnani College of Pharmacy, 23 Jote Joy, R. S. Marg, Cuffe Parade, Mumbai 400005, India.*

^b *School of Science, Monash University Malaysia Campus, Jalan Lagoon Selatan, Bandar Sunway, 47500, Selangor, Malaysia.*

*gurjar_a_s@yahoo.co.in

Abstract: Alzheimer's disease (AD) is a progressive neurodegenerative disorder with multiple factors associated with its pathogenesis. Our strategy against AD involves design of multi-targeted 2-substituted-4,5-diphenyl-1H-imidazole analogues which can interact and inhibit AChE, thereby, increasing the synaptic availability of ACh, inhibit BuChE, relieve induced oxidative stress and confer a neuroprotective role. Molecular docking was employed to study interactions within the AChE active site. *In silico* ADME study was performed to estimate pharmacokinetic parameters. Based on computational studies, some analogues were synthesized and subjected to pharmacological evaluation involving antioxidant activity, toxicity and memory model studies in animals followed by detailed mechanistic *in vitro* cholinesterase inhibition study. Amongst the series, analogue **13** and **20** are the most promising multi-targeted candidates which can potentially increase memory, decrease free radical levels and protect neurons against cognitive deficit.

Keywords: Acetylcholinesterase; 2-substituted-4,5-diphenyl-1H-imidazole; Molecular docking; *in vitro* antioxidant assay; *in vitro* Ellman assay.

1. Introduction

Alzheimer's disease (AD) is one of the most common neurodegenerative disorder mainly disrupting communication within neural circuits vital for memory and other cognitive functions.¹⁻² Past two decades have witnessed extensive research dedicated to unravel the molecular, biochemical, and cellular mechanisms of cognitive deficit.³ Various hypotheses have been proposed in the pathogenesis of AD like Acetylcholine (ACh) imbalance, amyloid beta ($A\beta$) production and its aggregation, tau hyperphosphorylation, oxidative stress and others including dysfunctional calcium homeostasis, hormonal, inflammatory-immunological causes. Hence, the development of an effectual therapeutics is of extreme importance.⁴

The deficiency of neurotransmitter ACh in the brain is a crucial factor associated with AD pathogenesis. 'Cholinergic hypothesis' states severe failure of cholinergic function in the central nervous system which contributes to cognitive symptoms. Acetylcholinesterase (AChE) or true ChE predominantly hydrolyzes ACh and is found in high concentrations mainly in the cholinergic brain synapses, at neuromuscular junctions and red blood cells. Butyrylcholinesterase (BuChE) or pseudo/plasma ChE is a non-specific type of cholinesterase enzyme that hydrolyzes different types of choline esters and exists ubiquitously throughout the body, most importantly, in the human liver, blood serum, pancreas and the central nervous system.⁵ BuChE mostly hydrolyzes ACh in later stages of AD due to increased BuChE activity and decreased AChE activity, so search of BuChE inhibitors for progressed AD patients can be beneficial.⁶ However, the most promising approach for symptomatic relief of AD is to inhibit the AChE, which primarily catalyzes the hydrolysis of ACh, thereby increasing synaptic levels of ACh in the brain. Research so far has not led to breakthrough drug candidate or a single pathway that can cure AD. Till date four acetylcholinesterase inhibitors such as tacrine, rivastigmine, galantamine,

donepezil and NMDA receptor antagonist memantine are the only US FDA approved drugs for its treatment.⁷⁻⁹

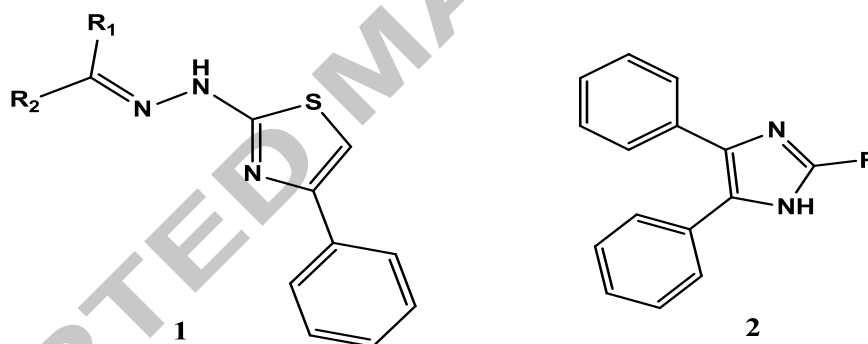
A unique structural aspect of AChE is a deep and narrow gorge, about 20Å long, which penetrates more than halfway and widens out at its base, where the catalytic triad lies.¹⁰ The peripheral anionic site (PAS) is located at the gorge entry lined by highly conserved 14 aromatic amino acid residues.¹¹ The X-ray crystallographic structure of AChE (PDB ID: 1EVE) has revealed the main binding sites i.e. esteratic subsite (catalytic triad) at the bottom of gorge (Ser200, His440, and Glu327); peripheral anionic site (PAS) with Tyr70, Asp72, Tyr121, Trp279 and Tyr334; an anionic substrate (AS) binding site having Trp84, Tyr130, Phe330 and Phe331, oxyanion hole with Gly118, Gly119, Ala201 and an acyl pocket (Phe288, and Phe290).¹²

In the literature, a new non-cholinergic role of AChE has been suggested; the enzyme co-localizes through its peripheral anionic site with the Aβ peptide deposits in the brain of AD patients and promotes Aβ fibrillogenesis by forming stable AChE-Aβ complexes, so inhibition of AChE will deter the fibrillogenesis.¹³⁻¹⁴ The accumulation of Aβ in various areas of the brain exhibits its neurotoxic effects through inflammation, calcium dysregulation and activating microglial cells which in turn cause oxidative stress and neuronal death.¹⁵ Due to the connection of various factors in the disease progression, modulation of a single aspect might not be satisfactory to achieve desired effectiveness. This has triggered our curiosity towards the design of multi-targeted analogues which can interact with both the catalytic triad and peripheral binding sites of AChE, thereby, increasing the synaptic availability of ACh, declining the deposition of Aβ, relieving induced oxidative stress and conferring a neuroprotective role.

Literature survey indicates that series developed possessing various heteroaromatic rings like coumarin, benzimidazole, thiazole, piperidine, indanone, spiro-indenoquinoxaline, spiro-

dihydropyridines derivatives showed promising acetylcholinesterase inhibitory activity.¹⁶⁻²¹ Rahim *et al* reported a series of thirty thiazole analogues (**1**) developed using structural-based drug design tool and evaluated their AChE and BuChE inhibitory potential. All analogues exhibited inhibition with an IC₅₀ value ranging from 1.59±0.01 to 389.25±1.75µM with an improvement in memory as well as cognitive functions including lowering of progressive neurodegeneration.²² Prompted by these findings we replaced the sulphur moiety of thiazoles with nitrogen and explored the imidazole scaffold and developed a series of 2-substituted-4,5-diphenyl-1H-imidazole analogues (**2**) to target multiple factors simultaneously involved in the etiopathogenesis of AD (**Figure 1**).

Figure 1: Substituted thiazole and 2-substituted-4,5-diphenyl-1H-imidazole scaffolds.



In this paper, we discuss computational studies which includes molecular docking within AChE active site and *in silico* ADME studies, synthesis, evaluation of antioxidant activity, toxicity and memory model studies in animals as well as *in vitro* cholinesterase inhibition activity of 2-substituted-4,5-diphenyl-1H-imidazole analogues.

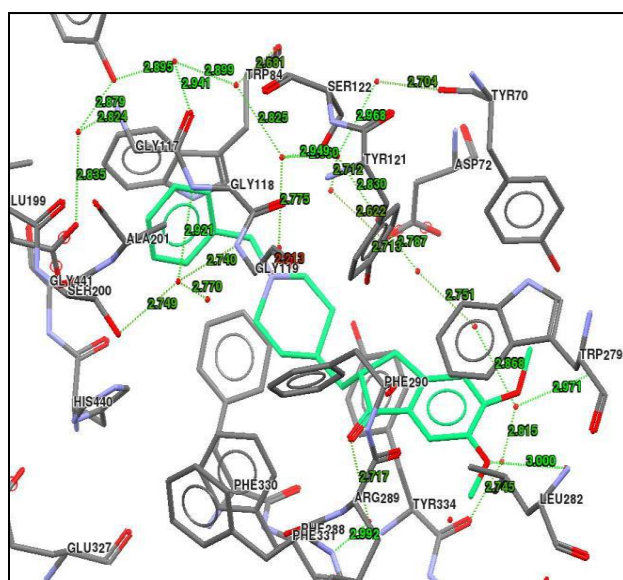
2. Results and discussion

2.1. Molecular Docking studies with AChE enzyme

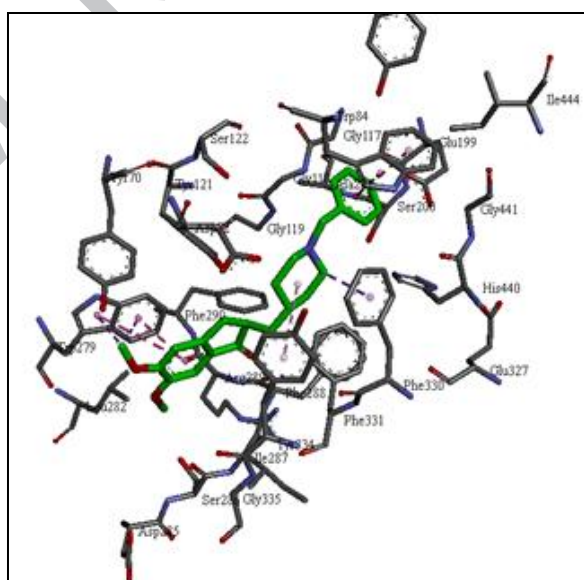
In the current study, docking approach has been utilized to explore the AChE active site, foresee orientation (pose) of the designed ligands in the binding pocket and assess the tightness of target-ligand interactions (scoring) using GOLD (Genetic Optimization for Ligand Docking) program with full range of ligand conformational flexibility and selective rotational flexibility of the receptor.²³⁻²⁴ The docking protocol was validated by reproduction of binding pose of the co-crystallized ligand donepezil in the enzyme active site (PDB: 1EVE; rmsd: 0.600). To further substantiate the protocol, some reported AChE inhibitors (AChEIs): Physostigmine (IC_{50} 0.220 μ M), Galantamine (IC_{50} 0.623 μ M), Alfuzosin (IC_{50} 0.018 μ M), Dyclonine (IC_{50} 0.181 μ M), Nefazodone (IC_{50} 1.037 μ M), Indanone derivatives (IC_{50} 0.0018 μ M) were also docked within the active site.²⁵⁻²⁸

The active marketed drug donepezil spans the entire gorge while the docked reported AChEIs occupy bottom and entrance of the gorge. Donepezil exhibited hydrogen-bond interactions through water molecules with the various active site residues such as Tyr70, Asp72, Trp84, Gly117, Tyr121, Ser122, Tyr130 and Ser200. Hence, water molecules play a crucial role in drug receptor interactions.²⁹ Also; the cyclic ketone group of indanone moiety depicted hydrogen-bond interaction with the Phe288 residue of the acyl pocket. The benzyl ring and indanone ring of donepezil displayed a classical π - π stacking with the indole ring of Trp84 and Trp279 respectively. N-benzyl piperidine fragment displayed π -sigma interaction with aromatic ring of Phe330. Similarly, methoxy group exhibited π -sigma interaction with indole ring of Trp279. π -alkyl interaction of the piperidine nitrogen was observed with Tyr334 residue of the active site. These results indicate positively that the docking protocol was able to acceptably

2a: H-bond formation



2b: Hydrophobic interactions



Subsequently, a series of 2-substituted-4,5-diphenyl-1H-imidazole analogues (**Table 1**) was docked in the AChE active site. The test analogues have reached bottom of the gorge and formed hydrogen bonds through water molecules with similar amino acid residues as observed for donepezil. The docking analysis revealed that imidazole analogues interact with active site primarily through hydrogen bonds and hydrophobic interactions such as pi-pi stacking, pi-pi

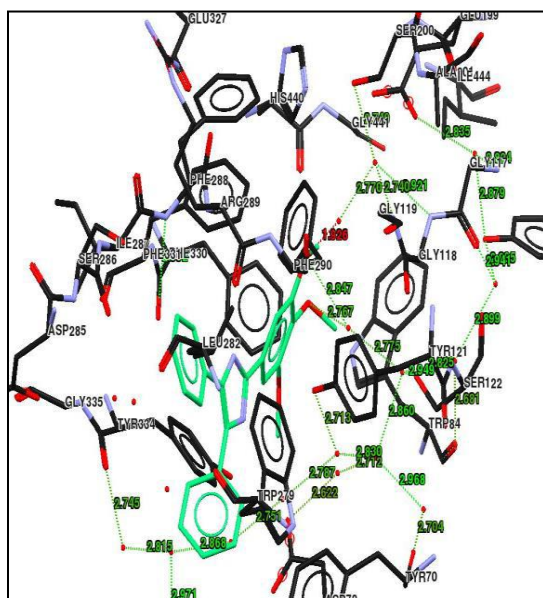
stacking (T-shaped), pi-sigma, pi-alkyl. Mostly the interactions of ligands were observed with residues present at bottom or middle of the gorge i.e with the catalytic triad (Ser200) and PAS (Tyr70, Asp72, Tyr121 and Tyr334). Anne Imberty *et al* related the distance of hydrogen bonds between a ligand and receptor with the type such as strong, average and weak interactions.³⁰ Results of imidazole analogues depicted that hydrogen bond interactions were of strong or average nature. In the designed test series, substituents have been varied at the 2-position in the imidazolyl ring system from simple alkyl groups such as methyl, ethyl to phenyl and heteroaryl. Further, the phenyl ring has been substituted with mono-, di-, and tri-substitutions of different functional groups such as nitro, hydroxyl, methoxy, amino and halogens. In case of 2-hydrogen and 2-methyl substituted analogues, interactions were mainly observed through the imidazole ring nitrogen with active site residues Tyr121 and Tyr334. However, on increasing the carbon chain length to ethyl and n-propyl showed no contacts. On substituting 2-position of imidazole ring with heteroaryl furan group, depicted interaction with indole ring nitrogen of Trp279 while phenyl ring substitution exhibited interaction with only one water molecule. Interestingly, on substituting the 2-phenyl ring with various functional groups depicted increased interactions with AChE active site residues. Now, instead of the imidazole ring nitrogen, the functional groups were involved in the interactions. On substituting 2-phenyl ring with electron withdrawing group such as nitro displayed less number of hydrogen bonds (Tyr70, Asp72 and Tyr121) whilst, electron donating groups such as hydroxy and methoxy groups not only increased the number of interactions but also exhibited hydrogen bonds with catalytic triad (especially Ser200) an important active site residue for enzymatic machinery. The halogens (-Cl, -F) and amino group substitution on 2-phenyl ring of imidazole displayed no contacts. A better insight of effect of substitution pattern on number of interactions was observed in case of methoxy substituted

analogues. Trisubstituted methoxy derivative exhibited highest number of hydrogen bonds as compared to disubstituted and monosubstituted methoxy analogues as well as compared with other analogues in the series. The 2-phenyl ring trisubstituted methoxy analogue interacted with Tyr70, Asp72, Trp84, Gly118, Gly119, Ser122, Tyr130 and Ser200 residues.

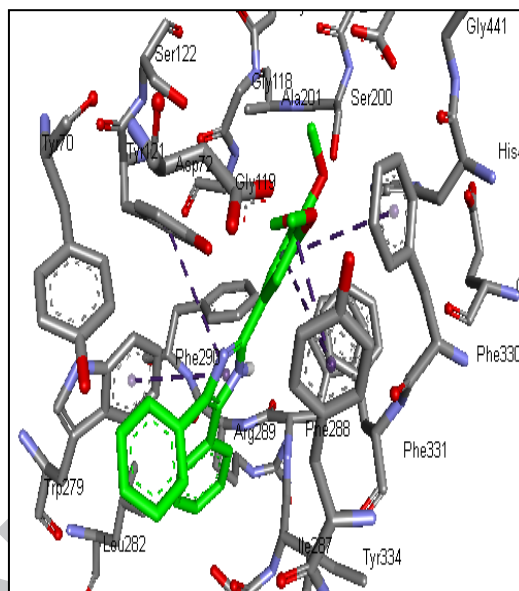
The analogues showing more interactions within AChE active site were remarkably found to interact with one of the catalytic triad residue Ser200 like donepezil. Amongst them notable observation was found for the methoxy substituted analogues. Specifically, the analogues **17**, **18**, **19** and **20** have shown increase in number of interactions with increase in number of methoxy group substitutions. The phenyl ring of imidazole substituted with polarizable group especially hydroxy has shown interaction with Ser200 which is important for enzymatic catalysis (analogue **13**). Thus, in the designed series, imidazole analogues possessing 2-phenyl ring substituted with methoxy or hydroxy group can be considered as more promising AChE inhibitors. The docking pose and hydrophobic interactions of representative analogue **20** have been depicted in **Figure 3a&b**.

Figure 3 a&b: Docking pose of analogue 20 within AChE active site

3a: H-bond formation



3b: Hydrophobic interactions



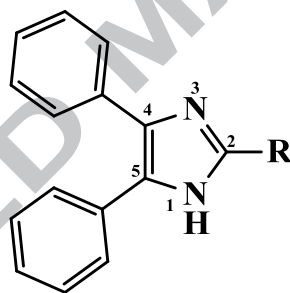
2.2. *In silico* ADME studies

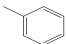
Drug kinetics and exposure of tissues to drug influences the pharmacological activity and the performance of a drug candidate, which is eventually determined by its ADME properties. The ultimate objective of the *in silico* ADME studies is to accurately predict *in vivo* pharmacokinetics of a possible and potential drug molecule.³¹ Results of *in silico* ADME descriptors calculated for the 2-substituted-4,5-diphenyl-1H-imidazole analogues using QikProp software of Schrodinger have been depicted in **Table 1**.

ADME results for CNS parameter seem to be favourable and indicate that all analogues can be targeted for CNS activity. All the designed analogues were small in size with molecular weight less than 400 g/mol, donor HB (hydrogen bond) upto 3 and acceptor HB in the range of 2-4. Solvent Accessible Surface Area (SASA) can be used as a size related parameter which affects the partition co-efficient and aqueous solubility which was observed to be in the range of 400-800.³² The QPlogPo/w is a significant aspect to determine bioavailability and seems to be

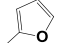
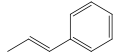
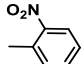
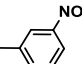
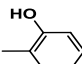
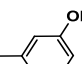
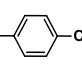
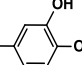
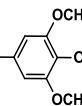
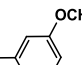
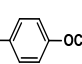
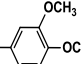
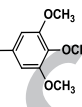
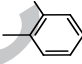
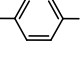
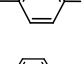
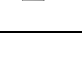
favourable. Further, the predicted values for blood–brain barrier (BBB) penetration (QPlogBB) of all analogues were in the optimum range (–3 to 1.2). The QPPMDCK model is considered to be a good mimic for the blood-brain barrier. The QPPMDCK descriptor values were found to be great for most of the analogues whilst analogue **11** and **15** had moderate values. The percent human oral absorption was found to be more than 90% for all analogues. None of these imidazole analogues violated the Lipinski's rule of five, thus interpreting these analogues as suitable drug candidates. Overall, *in silico* ADME results indicate that all analogues can be thought to be CNS active and the descriptor values were found to be in the QikProp specified ranges so these analogues seem to possess favourable pharmacokinetic properties.³³

Table 1: *In Silico* ADME results of 2-substituted-4,5-diphenyl-1H-imidazole analogues



No	R	CNS	MW ^a	donor HB	accpt HB	SASA	QPlog Po/w	QPlog BB	QPPMDCK	% Human Oral Absorption	Rule Of Five
3	H	1	220.27	1	1.5	465.52	3.66	0.21	2284.05	100	0
4	CH ₃	1	234.30	1	1.5	502.99	4.12	0.30	2982.82	100	0
5	CH ₂ CH ₃	1	248.33	1	1.5	535.29	4.56	0.30	3539.05	100	0
6	CH ₂ CH ₂ CH ₃	1	262.35	1	1.5	560.43	4.93	0.34	3952.59	100	0
7		1	296.37	1	1.5	593.10	5.59	0.41	4114.49	100	1

(Continued on next page)

8		1	286.33	1	2	555.90	4.92	0.36	3557.92	100	0
9		1	398.51	1	1.5	771.53	7.96	0.21	4113.17	100	1
10		0	341.37	1	2.5	627.57	5.02	-0.46	618.42	100	1
11		0	341.37	1	2.5	631.08	4.89	-0.63	415.02	100	0
12		0	312.37	2	2.25	605.31	4.87	-0.06	1540.05	100	0
13		0	312.37	2	2.25	605.54	4.77	-0.18	1135.48	100	0
14		0	312.37	2	2.25	605.52	4.77	-0.19	1131.78	100	0
15		-1	328.37	3	3	616.49	4.02	-0.72	377.29	100	0
16		0	372.42	2	3.75	674.38	5.15	-0.12	1875.21	100	1
17		1	326.40	1	2.25	630.10	5.69	0.35	4117.04	100	1
18		1	326.40	1	2.25	629.90	5.70	0.35	4112.43	100	1
19		1	356.42	1	3	673.10	5.88	0.28	4114.65	100	1
20		1	386.46	1	3.75	698.17	5.93	0.22	4108.68	100	1
21		2	330.82	1	1.5	604.92	5.94	0.50	7236.91	100	1
22		2	330.82	1	1.5	617.18	6.09	0.59	10000	100	1
23		2	314.36	1	1.5	602.15	5.83	0.53	7445.97	100	1
24		1	339.44	1	2.5	670.64	6.04	0.33	3961.24	100	1

^a gm/mol

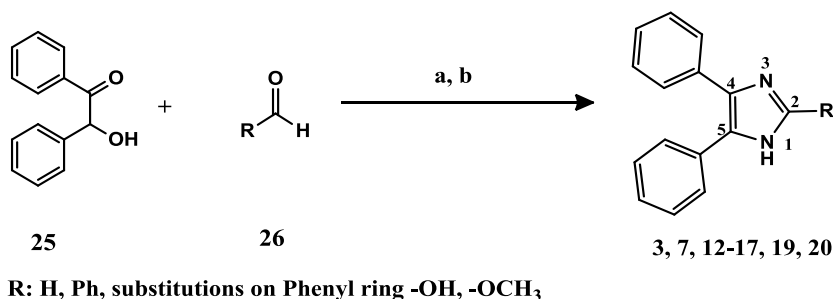
2.2.1 Correlation of *in silico* ADME studies with docking results

Molecular docking results have been found to be in consensus with the predicted *in silico* ADME data. It shows that the analogues substituted with polarizable groups such as hydroxy, methoxy on 2-phenyl ring have displayed maximum number of interactions and analogously favourable CNS parameters and high human oral absorption. These analogues were subjected to synthesis and further studies.

2.3 Synthesis

Based on the outcome of the computational studies from the series consisting of 24 analogues, 10 compounds were further synthesized using ceric ammonium nitrate as catalyst³⁴ (**Scheme 1**). The synthesized and purified analogues were characterized by spectral techniques: IR, ¹HNMR, ¹³CNMR and Mass spectroscopy. Purity of analogues was estimated using HPLC technique. The IR spectra of the synthesized analogues depicted expected absorption bands for the functional groups. The formation of imidazole ring was revealed by the presence of singlet near 12 ppm and also exhibited predictable delta values for all other aliphatic and aromatic protons in ¹HNMR spectra. Thus, the spectroscopic techniques confirmed the correctness of anticipated structures of the synthesized analogues.

Scheme1^b: General reaction for synthesis of 2-substituted-4,5-diphenyl-1H-imidazole



^b Reagents: (a) Ceric Ammonium nitrate (10 mol%); (b) Ammonium acetate (40 mmol); Ethanol-water reflux(24-48 hrs.)

2.4 Pharmacological evaluation

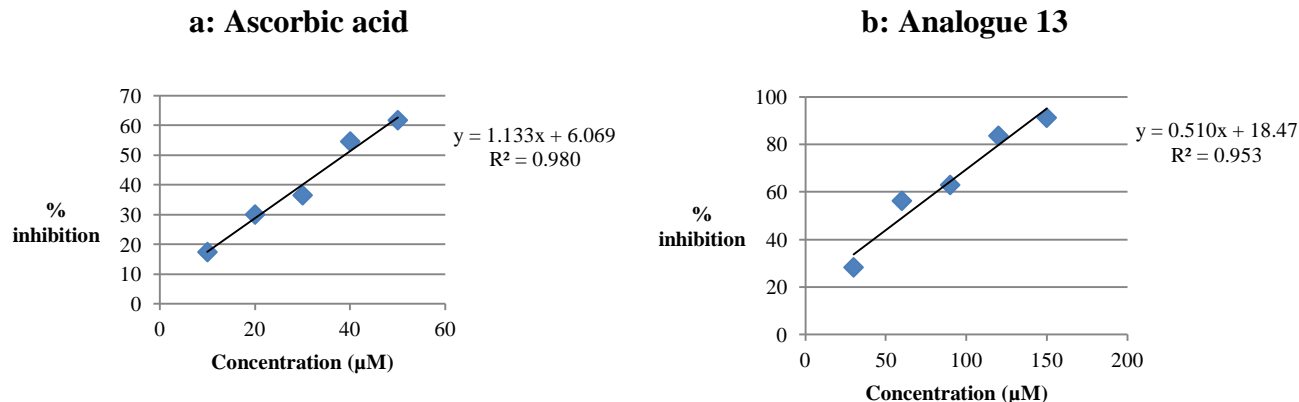
2.4.1 *In vitro* lipid peroxidation (LPO) assay

Oxidative stress and A β -accumulation leads to formation of lipid peroxidation product malondialdehyde. Hence, anti-oxidant activity was determined by carrying out *in vitro* lipid peroxidation (LPO) assay.^{35, 36} For the comparison of *in vitro* LPO assay results, ascorbic acid was considered as the reference compound. The IC₅₀ values for antioxidant activity of all the synthesized imidazole analogues were estimated and found to be in the range of 59-264 μ M (**Table 2**). Amongst the series, analogue **15** exhibited maximum antioxidant activity followed by analogue **20** and **13**. These analogues possessed primarily hydroxy and methoxy groups as substituents in the 2-phenyl ring. From the structure-activity relationship (SAR) point of view it can be proposed that as analogue **15** possesses more hydroxyl groups so it can hinder the oxidation process more effectively than the corresponding monohydroxy as well as methoxy analogues. Graphs of the LPO assay results of reference compound and representative analogue **13** are depicted in **Figure 4**. Thus, overall *in vitro* LPO assay results showcase the neuroprotective role of these analogues.

Table 2: *In vitro* LPO assay results

Analogues	IC ₅₀ (μ M) ^c
3	93.24
7	106.05
12	100.84
13	61.82
14	62.37
15	59.42
16	264.31
17	86.46
19	94.01
20	61.29
Ascorbic acid	38.77

^c Values are the mean values of at least two experiments

Figure 4: LPO inhibitory assay for ascorbic acid (a) and analogue 13 (b)

2.4.1.1 Correlation of *in vitro* LPO assay and computational studies

Comparison between docking and *in vitro* LPO assay results highlighted analogues **13**, **14**, **15**, **19** and **20** in the series. These analogues exhibited good number of hydrogen bond and hydrophobic interactions within AChE active site. Amongst these analogues; **13**, **19** and **20** interacted with one of the residues of catalytic triad (Ser200) of AChE which plays a fundamental role in enzymatic catalysis and inhibitor binding. The IC₅₀ value for analogue **19** was no doubt higher than the above highlighted ones but it depicted interaction with crucial catalytic triad residue of AChE enzyme. The LPO assay result of analogue **19** was comparable to analogues **3** and **7** but they did not exhibit good docking results as observed with analogue **19**. The *in silico* ADME results were favourable but QPPMDCK value of analogue **15** was not found to be great. Collating all inputs analogue **13** and **20** were selected for further studies.

2.4.2 Acute toxicity studies

Oral administration of the representative test analogue **20** at the dose of 800 mg/kg did not reveal any signs of toxicity, behavioral changes or mortality in a group of 6 animals (3 male and 3 female Swiss albino mice) for 14 consecutive days, so the dose was considered to be safe and non-lethal. Various parameters studied for toxicological observations of the test analogue **20**

were awareness, mood, CNS excitation, CNS depression and autonomic reflexes. Further, on increasing the dose of analogue **20** to 900mg/kg resulted in 50% mortality in the group of six animals.

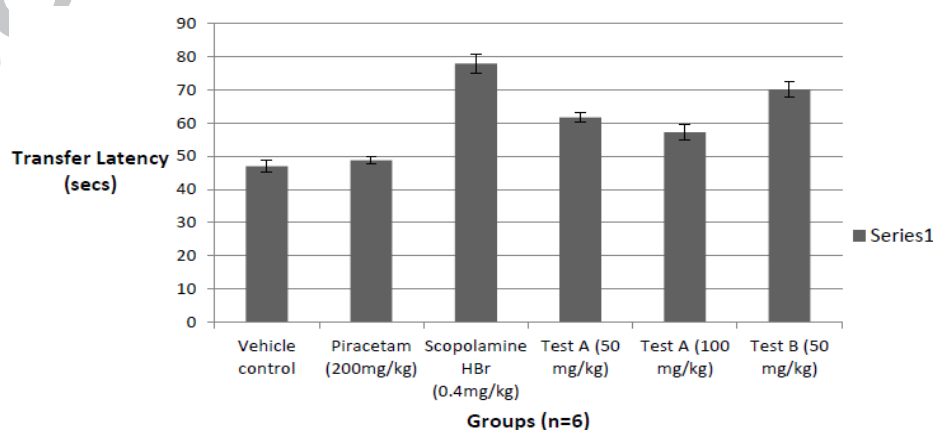
2.4.3 Memory model studies

The *in silico* ADME results indicated that all designed analogues of the 2-substituted-4,5-diphenyl-1H-imidazole series can be thought to be CNS active. To authenticate this finding, memory model studies were undertaken before venturing into the detailed mechanistic *in vitro* cholinesterase inhibition study.

2.4.3.1 Elevated Plus Maze (EPM) model

This model was used to evaluate memory and learning in Swiss albino mice. Decrease in transfer latency (TL) in seconds was observed for test analogues **20** (Test A) and **13** (Test B) as compared to the toxicant group (scopolamine hydrobromide) which conveys us that both the analogues were able to retain the memory of mice to travel in one of the closed arms of maze. Results of EPM demonstrate that both the analogues helped successfully to retain the memory in mice with values of analogue **20** close to the reference drug Piracetam (**Figure 5**).

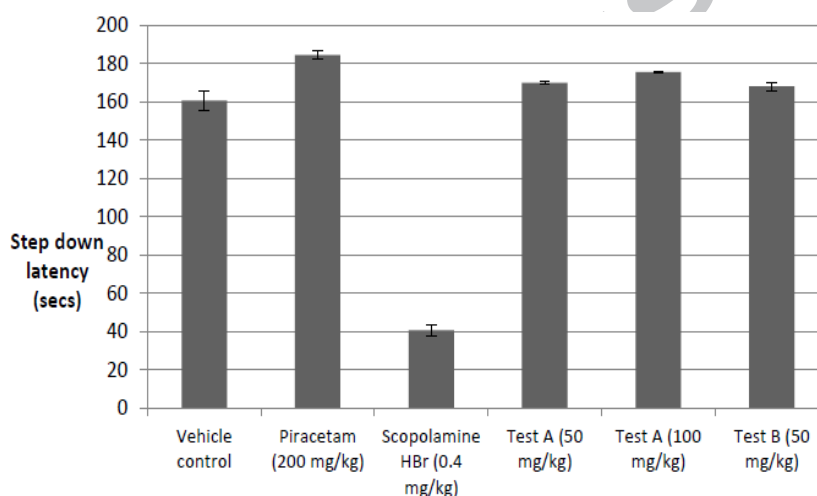
Figure 5: Effect of test analogues on Transfer Latency



2.4.3.2 Step down inhibitory avoidance test

Animals administered with test analogues **20** (Test A) and **13** (Test B) took more time to step down from the block as compared with toxicant which indicates memory retention in them. Results of step down inhibitory avoidance model ascertain that both the analogues helped effectively to retain the memory and learning in mice very much close to the standard Piracetam drug whilst very much distant from the toxicant scopolamine results (**Figure 6**).

Figure 6: Effect of test analogues on Step Down Latency



Data of EPM and step down inhibitory avoidance model were analyzed by one-way ANOVA. A significant statistical difference was found between control and test groups (p value > 0.05). So, Dunett multiple comparison tests as post-test was applied to the data. Thus, both the analogues **13** and **20** exhibited effective memory retention in the animals and can be considered as promising CNS target candidates.

2.4.4 *In vitro* cholinesterase inhibition

A total of ten synthesized 2-substituted-4,5-diphenyl-1H-imidazole analogues were screened at 10 μ M concentration using Ellman's method to test their effectiveness in cholinesterase inhibition (AChE and BuChE). Thereafter, IC₅₀ values of analogues which

exhibited more than 50% inhibition at 10 μ M concentration were estimated and compared with reference drugs Donepezil and Galantamine for AChE and BuChE respectively (**Table 3**). Previous results from computational and *in vitro* pharmacological evaluation studies furnished five promising imidazole analogues (**13**, **14**, **15**, **19** and **20**). These are mainly analogues which possess 2-phenyl ring substituted with either methoxy or hydroxy group. This indicates that electronic effect predominates in the SAR of the series. Analogue **13** and **19** were found to be the most potent inhibitors for AChE in the series. In comparison, analogue **13** was deemed a better candidate as analogue **19** had poor aqueous solubility. For BuChE inhibition assay, the results demonstrated that multiple substitutions on the 2-phenyl ring gave better BuChE inhibitory activity as compared to mono substitution, with analogue **20** to be the most potent one (**Table 4**).

Table 3: AChE and BuChE inhibition results

Analogue	% AChE inhibition \pm SD at 10 μ M ^d	% BuChE inhibition \pm SD at 10 μ M ^d
3	39.70 \pm 3.44	13.01 \pm 1.99
7	16.08 \pm 2.52	N.I.
12	15.08 \pm 2.60	13.70 \pm 1.82
13	65.08 \pm 4.34	N.I.
14	6.53 ^e	N.I.
15	N.I.	79.45 \pm 6.60
16	29.65 \pm 2.01	N.I.
17	23.62 \pm 3.45	19.18 \pm 3.66
19	67.33 ^e	N.I.
20	N.I.	81.28 \pm 6.85
Donepezil	91.07 \pm 8.23	N.D.
Galantamine	N.D.	80.77 \pm 8.01

^d Experiments were carried out in quadruplicate and repeated at least twice; ^e Precipitation was observed at 10 μ M (1% DMSO), N.I. No inhibition, N.D. Not determined

Table 4: IC₅₀ values of the most potent AChE and BuChE inhibitor.

Analogue	AChE inhibition IC ₅₀ (μM) ^f	BuChE inhibition IC ₅₀ (μM) ^f
13	5.33	N.I.
20	N.I.	4.99
Donepezil	0.1	N.D.
Galantamine	1.67	3.31

^fExperiments were carried out in quadruplicate and repeated at least twice
N.I. No inhibition, N.D. Not determined

2.4.5 Structure activity relationship

Imidazole scaffold is the core moiety of the designed series. The improvements in the activity can be achieved by modifications on the imidazole nucleus. Incorporation of phenyl rings may provide additional hydrophobic sites for interaction between inhibitor and the enzyme. Hence, phenyl rings were substituted at 4th and 5th position of imidazole ring. Structure activity relationship analysis reveals that AChE inhibition potency is closely related to the substitution at 2-position of imidazole core. Analogues with various substituents such as electron-withdrawing, electron-donating were considered. Altering substituents at the 2-position of imidazolyl nucleus from simple alkyl groups such as methyl, ethyl to aryl and heteroaryl led to varying consequences on binding and inhibitory activity. Substituting hydrogen and methyl group at 2-position, showed lesser docking interactions and gave comparable LPO assay results. However, on increasing the carbon chain length to ethyl and n-propyl showed no contacts within AChE active site. Also substituting aryl ring with halogens (-Cl, -F) and amino group did not furnish noteworthy docking results.

Interestingly, on substituting the 2-phenyl ring with various polarisable groups depicted increased interactions with AChE active site residues. Substituting electron-donating hydroxy group at 2nd/3rd/4th position of 2-phenyl ring (analogue **12**, **13** and **14**) displayed good interactions as compared to electron-withdrawing nitro group (analogue **10**, **11**). Further, incorporation of additional hydroxy group (analogue **15**) exhibited maximum antioxidant activity. Dihydroxy analogue can hinder the oxidation process more effectively as compared to monohydroxy analogues and analogously exhibited better LPO assay results.

A better insight of effect of substitution pattern on number of interactions was observed on inclusion of methoxy group at 2-phenyl ring. Trisubstituted methoxy analogues (analogue **20**) gave better docking results and antioxidant activity as compared to mono- and di-substituted methoxy candidates. Monohydroxy analogues were found to have affinity towards AChE while dihydroxy analogues selectively inhibited BuChE. It was interestingly noted that increasing the number of substitutions led to selectivity and affinity towards BuChE. Accordingly, the trisubstituted analogue **20** exhibited maximum BuChE inhibitory activity. Analogue **13** and **19** were found to be the most potent inhibitors for AChE in the series. Those analogues possessing primarily hydroxy and methoxy groups as substituents in the 2-phenyl ring can be considered as potential lead for further optimization and development of more promising imidazole analogues with multiple roles of cholinesterase inhibition, antioxidant effect and neuroprotection.

3. Conclusion

In the designed 2-substituted-4,5-diphenyl-1H-imidazole series, the analogues chosen for synthesis exhibited more number of interactions with AChE active site residues, interacted with the catalytic triad and PAS; significant for enzymatic catalysis, showed favourable pharmacokinetic properties, depicted neuroprotective effect against oxidative stress with

retention of memory in memory model studies as well as inhibited the AChE enzyme at 10 μ M concentration. Thus, it can be foreseen that the synthesized 2-substituted-4,5-diphenyl-1H-imidazole analogues can potentially increase memory, decrease free radical levels and protect neurons against cognitive deficit. Therefore, amongst the series, analogue **13** can be considered as potential lead for further optimization and development of more promising imidazole analogues with multiple roles of AChE inhibition, antioxidant and neuroprotection. Further, analogue **20** can be explored for search of newer BuChE inhibitors. This biological profile highlights the importance of these analogues as promising multi-targeted prototypes in the search of new protective and regenerative drugs for the potential treatment of Alzheimer's disease.

4. Materials and Method

4.1. Molecular Docking studies with AChE enzyme

4.1.1. Materials

Sybyl version 8.1.1 (Tripos International, Portugal) running on Red Hat Enterprise Linux (RHEL) workstation was utilized for ligand preparation and its Biopolymer module for protein preparation.³⁷ GOLD version 5.2.2 (CCDC Ltd., UK) running on RHEL workstation was employed to carry out docking studies.³⁸

4.1.2. Structure based designing of ligands

All the structures of reported AChE inhibitors and test ligands of imidazole series were sketched and subjected to energy minimization using steepest descent (SD) and Powell methods with TRIPOS force field to attain gradient convergence of 0.0001 kcal/mol/Å. Gasteiger-Hückel partial atomic charges were assigned to all compounds.

4.1.3. Preparation of protein for docking

The x-ray crystal structure of enzyme AChE (PDB ID: 1EVE, resolved at 2.5Å) complexed with the ligand Donepezil was retrieved from protein data bank for structure aided drug design.¹² The ligand donepezil was extracted along with undesired water molecules, hydrogen atoms were added, atom types and partial charges were assigned. Based on site points of the complexed ligand, active site of protein was defined and confirmed from literature. The active site was defined as a sphere with a radius of 7Å from the bound ligand which was found to be equivalent to 10Å in GOLD. 20 key structural water molecules were retained in the active site. The side chains were subjected to minimization using AMBER7FF99 force field to a gradient of 0.001 kcal/mol/Å.^{12, 38}

4.1.4. Docking protocol

The refined protein, minimized reported ligands and imidazole analogues were imported into GOLD. The default parameters in GOLD v5.2.2 were utilized for docking studies. Docking was carried out for 20 genetic algorithm (GA) runs with 1,00,000 operations and GoldScore as the fitness function. The docking protocol was validated by reproduction of the binding pose of donepezil in 1EVE. Further, the protocol was substantiated by docking reported AChEIs within the active site. The best ranked pose of ligands was studied to determine their binding as well as interactions within the AChE active site.

4.2. In silico ADME studies

4.2.1. Materials

In silico ADME studies were carried out with QikProp version 3.3 (Schrodinger LLC, New York, USA) software running on Red Hat Enterprise Linux (RHEL) workstation.³³

4.2.2. Method

Each designed structure was optimized by LigPrep using OPLS-2005 force field. Out file of LigPrep was used as input file for QikProp to determine various pharmacokinetic descriptors. QikProp jobs were monitored and results were obtained in the form of OUT file.

4.3 Synthesis

4.3.1 Materials

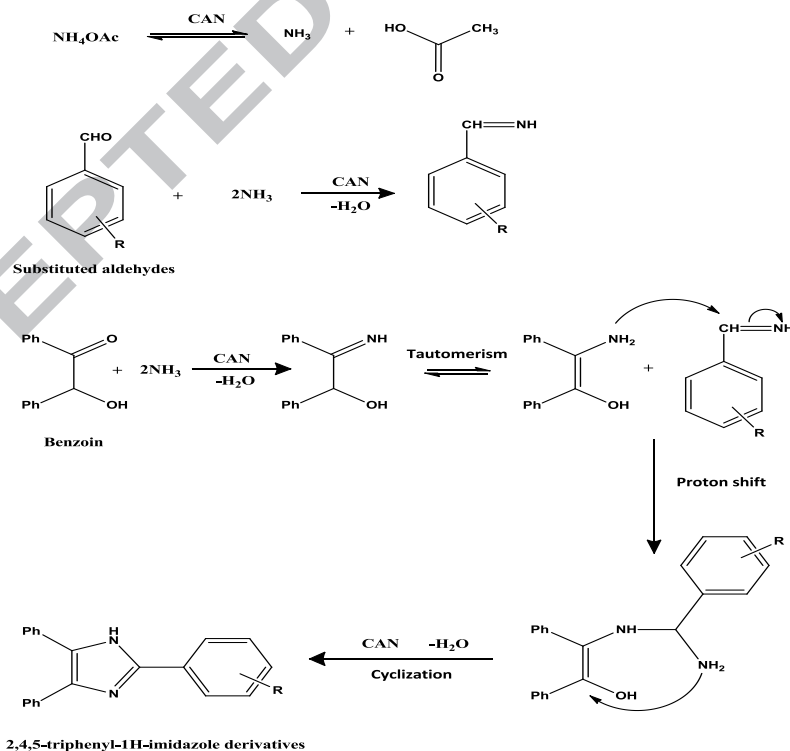
All chemicals and solvents used were obtained from commercial sources. The starting materials were assessed for purity by physical constant determination and thin layer chromatography (TLC) on Merck silica gel F₂₅₄ plates. TLC was employed to monitor all reactions. Physical constants were determined in Analab melting point apparatus μ ThermoCal10. Infrared (IR) spectra were recorded on Shimadzu IR 8400S. ¹HNMR, ¹³CNMR spectra's in DMSO (Dimethyl sulfoxide) solvent were recorded on Mercury Plus 300 MHz (Varian, USA) NMR Spectrometer. Chemical shifts have been reported in parts per million (ppm) using tetramethylsilane (TMS) as an internal standard. Mass spectra were obtained using 410 Prostar Binary LC with 500 MS IT PDA detectors (Varian Inc, USA) mass spectrometer. Percent purity of samples was obtained using HPLC technique by Agilent 1200 Series HPLC System.

4.3.2 General procedure

A mixture of benzoin (**25**, 10 mmol), ceric ammonium nitrate (10 mol %) and ammonium acetate (40 mmol) was dissolved in ethanol-water (20 ml, 1:1 v/v) and substituted aldehyde (**26**, 10 mmol) was added to reaction mixture. This was subjected to reflux (75-80 °C) till completion of the reaction as indicated by TLC. The reaction mixture was allowed to cool to room temperature and then poured on ice-water to precipitate the solid compound. The crude product

was filtered and washed with water to free from impurities. It was purified by dissolving in dimethyl sulfoxide and the solution was poured on ice with stirring to precipitate the desired product. Further, purification was done by recrystallisation using ethanol or column chromatography (n-hexane: Ethyl acetate, 7: 3). All synthesized analogues were characterized using IR, ^1H NMR, ^{13}C NMR and Mass spectroscopy. Purity of compounds was assessed by HPLC technique. HPLC was performed using Inertsil-C18 reverse phase column (0.46×25 cm) on instrument equipped with an automatic injector with UV-PDA detector. The mobile phase consists of 0.05% TFA and acetonitrile (1:1, v/v). Products were eluted at flow rate of 1 ml/min using isocratic method. Detection was carried out at 254 nm. The melting points were also recorded. The plausible mechanism has been depicted in **Scheme 2**.

Scheme 2: Plausible reaction mechanism for synthesis of 2-substituted-4,5-diphenyl-1H-imidazole analogues



4.3.3 Spectral and analytical data

1. 4,5-diphenyl-1H-imidazole (3): White solid, Yield: 97.08%; 226.4⁰C, HPLC purity: 98.69%.

FTIR (cm⁻¹): 3447 (NH), 3134 (C-H), 1493(C=C), 1400 (C-N), 1630 (C=N); ¹H NMR (300 MHz, DMSO-d₆): δ 12.770 (s, 1H), 8.252 (s, 1H), 7.744-7.762 (d, 4H, J=6.4 Hz), 7.353-7.330 (d, 4H, J=6.690 Hz), 7.465-7.404 (d, 2H, J=8.32 Hz); ESI-MS (acetone) [M+1]: 221.3

2. 2,4,5-triphenyl-1H-imidazole (7): Off-white solid, Yield: 79.13%; 272.3⁰C, HPLC purity:

98.45%. FTIR (cm⁻¹): 3445 (NH), 3082 (C-H), 1462(C=C), 1386 (C-N), 1641 (C=N); ¹H NMR (300 MHz, DMSO-d₆): δ 12.758 (s, 1H), 7.929-7.903 (d, 2H, J=7.7 Hz), 7.822-7.774 (t, 2H, J=7.3 Hz), 7.376-7.354 (d, 1H, J=6.6 Hz), 7.583-7.536 (d, 4H, J=7.0 Hz), 7.656-7.605 (t, 4H, J=7.7 Hz), 7.519-7.511 (d, 2H, J=2.6 Hz); ¹³C NMR (300 MHz, DMSO-d₆): δ 194.898, 135.611, 132.289, 129.646, 129.570, 129.273, 129.081, 128.813, 128.355, 127.741, 126.525, 126.180; ESI-MS (acetone) [M+1]: 297.4

3. 2-(2-hydroxyphenyl)-4,5-diphenyl-1H-imidazole (12): Yellowish solid, Yield: 69.38%;

206.8⁰C, HPLC purity: 99.34%. FTIR (cm⁻¹): 3416 (NH), 3175 (OH), 2926 (C-H), 1449 (C=C), 1398 (C-N), 1620 (C=N); ¹H NMR (300 MHz, DMSO-d₆): δ 12.651 (s, 1H), 10.268 (s, 1H), 7.802-7.776 (dd, 1H, J=2.3 Hz), 7.397-7.356 (t, 1H, J=6.2 Hz), 7.345-7.305 (t, 1H, J=5.8 Hz), 7.280-7.195 (dd, 1H, J=8.9 Hz), 7.979-7.935 (d, 2H, J=13.1 Hz), 7.910-7.905 (d, 2H, J=1.4 Hz), 7.632-7.607 (t, 2H, J=3.6 Hz), 7.521-7.484 (t, 2H, J=5.4 Hz), 7.600-7.545 (t, 1H, J=3.6 Hz), 7.472-7.424 (t, 1H, J=6.7 Hz); ¹³C NMR (300 MHz, DMSO-d₆): δ 194.851, 143.424, 138.024, 136.904, 135.564, 135.114, 132.251, 131.542, 130.230, 130.202, 129.666, 129.608, 128.766, 128.220, 127.205; ESI-MS (acetone) [M+1]: 313.3

4. 2-(3-hydroxyphenyl)-4,5-diphenyl-1H-imidazole (13): Brownish solid, Yield: 91.15%; 215.2^oC, HPLC purity: 97.81%. FTIR (cm⁻¹): 3441 (NH), 3132 (OH), 3233 (C-H), 1493 (C=C), 1402 (C-N), 1609 (C=N); ¹H NMR (300 MHz, DMSO-d₆): δ 12.758 (s, 1H), 8.357 (s, 1H), 7.455 (s, 1H), 7.430-7.404 (d, 1H, J=8.5 Hz), 7.374-7.348 (d, 1H, J=7.7 Hz), 7.159-7.137 (d, 1H, J=6.6 Hz), 7.298-7.260 (d, 6H, J=8.7 Hz), 7.244-7.195 (t, 4H, J=7.5 Hz); ¹³C NMR (300 MHz, DMSO-d₆): δ 177.24, 129.484, 128.354, 128.181; ESI-MS (acetone) [M+1]: 313.4

5. 2-(4-hydroxyphenyl)-4,5-diphenyl-1H-imidazole (14): Brown solid, Yield: 72.10%; 261.4^oC, HPLC purity: 97.44%. FTIR (cm⁻¹): 3449 (NH), 3179 (OH), 2857 (C-H), 1491 (C=C), 1398 (C-N), 1609 (C=N); ¹H NMR (300 MHz, DMSO-d₆): δ 12.429 (s, 1H), 9.755 (s, 1H), 7.782-7.736 (dt, 2H, 8.2 Hz), 6.938-6.909 (d, 2H, J=8.4 Hz), 7.934-7.905 (dd, 4H, J=1.0 Hz), 7.822-7.802 (d, 2H, J=6.2 Hz), 7.659-7.607 (t, 4H, J=7.7 Hz); ¹³C NMR (300 MHz, DMSO-d₆): δ 194.822, 135.535, 132.241, 129.589, 129.503; ESI-MS (acetone) [M+1]: 313.4

6. 2-(3,4-dihydroxyphenyl)-4,5-diphenyl-1H-imidazole (15): Dark brown solid, Yield: 68.83%; 226.8^oC, HPLC purity: 99.25%. FTIR (cm⁻¹): 3448 (NH), 3132 (OH), 3032 (C-H), 1628 (C=C), 1496 (C-N), 1628 (C=N); ¹H NMR (300 MHz, DMSO-d₆): δ 10.166 (s, 1H), 9.689 (s, 1H), 9.607 (s, 1H), 7.287-7.254 (dd, 1H, 4.5 Hz), 7.231-7.224 (d, 1H, 2.2 Hz), 6.916-6.889 (d, 1H, 8.0 Hz), 7.934-7.925 (d, 2H, 7.0 Hz), 7.910-7.905 (d, 2H, 7.0 Hz), 7.826-7.781 (t, 2H, 6.8 Hz), 7.657-7.607 (t, 2H, 7.5 Hz), 7.422-7.375 (dd, 2H, 6.9 Hz); ¹³C NMR (300 MHz, DMSO-d₆): δ 194.860, 146.910, 145.895, 145.521, 135.564, 132.270, 129.618, 129.531, 128.584, 128.095, 117.592, 115.744, 113.542; ESI-MS (acetone) [M+1]: 329.4

7. 2-(4-hydroxy-3,5-dimethoxyphenyl)-4,5-diphenyl-1H-imidazole (16): White solid, Yield: 72%; 225.8^oC, HPLC purity: 98.69%. FTIR (cm⁻¹): 3418 (NH), 3130 (OH), 1203, 1070 (C-O-

C), 2926 (C-H), 1485 (C=C), 1402 (C-N), 1605 (C=N); ^1H NMR (300 MHz, DMSO- d_6): δ 10.021 (s, 1H), 8.529 (s, 1H), 3.814 (s, 6H), 7.403-7.401 (d, 2H, 0.7 Hz), 7.609-7.551 (t, 2H, 8.6 Hz), 7.524-7.512 (d, 2H, 3.7 Hz), 7.503 (s, 2H), 7.287-7.277 (d, 2H, 2.9 Hz), 7.269-7.247 (t, 2H, 3.2 Hz); ^{13}C NMR (300 MHz, DMSO- d_6): δ 198.247, 198.055, 183.578, 176.972, 167.349, 166.660, 153.102, 152.489, 140.492, 138.864, 137.983, 137.926, 129.883, 129.672, 124.262, 124.071, 123.496, 122.616, 118.786, 118.039, 26.756, 13.878, 13.686; ESI-MS (acetone) $[M+]$: 372.4.

8. 2-(3-methoxyphenyl)-4,5-diphenyl-1H-imidazole (17): Yellow solid, Yield: 73.20%; 235.6 $^{\circ}\text{C}$, HPLC purity: 99.98%. FTIR (cm^{-1}): 3439 (NH), 1247, 1030 (C-O-C), 2985 (C-H), 1491 (C=C), 1402 (C-N), 1612 (C=N); ^1H NMR (300 MHz, DMSO- d_6): δ 12.677 (s, 1H), 2.386 (s, 3H), 7.375 (s, 1H), 7.821 (bs, 1H), 7.797-7.772 (d, 2H, 7.3 Hz), 7.927-7.902 (d, 6H, 7.7 Hz), 7.655-7.604 (t, 4H, 7.7 Hz); ^{13}C NMR (300 MHz, DMSO- d_6): δ 176.113, 152.386, 148.116, 148.068, 140.619, 139.064, 130.240, 130.087, 125.156, 124.688, 117.659, 116.720, 113.044, 112.527, 18.503; ESI-MS (acetone) $[M+]$: 326.7

9. 2-(3,4-dimethoxyphenyl)-4,5-diphenyl-1H-imidazole (19): Off-white, Yield: 79.04%; 217.2 $^{\circ}\text{C}$, HPLC purity: 98.88%. FTIR (cm^{-1}): 3418 (NH), 3132 (C-H), 1254, 1024 (C-O-C), 1497 (C=C), 1445 (C-N), 1607 (C=N); ^1H NMR (300 MHz, DMSO- d_6): δ 12.603 (s, 1H), 3.860 (s, 3H), 3.820 (s, 3H), 7.572-7.566 (d, 1H, 1.8 Hz), 7.545-7.539 (d, 1H, 1.8 Hz), 7.384-7.378 (d, 6H, 1.8 Hz), 7.180 (s, 4H), 7.153 (s, 1H); ^{13}C NMR (300 MHz, DMSO- d_6): δ 175.577, 129.618, 128.967, 128.316; ESI-MS (acetone) $[M+1]$: 357.4

10. 2-(3,4,5-trimethoxyphenyl)-4,5-diphenyl-1H-imidazole (20): White amorphous powder, Yield: 75.82%; 285.2 $^{\circ}\text{C}$, HPLC purity: 98.89%. FTIR (cm^{-1}): 2960 (NH), 1128, 1006 (C-O-C),

2934 (C-H), 1493 (C=C), 1464 (C-N), 1587 (C=N); ^1H NMR (300 MHz, DMSO- d_6): δ 11.884 (s, 1H), 3.863 (s, 3H), 3.853 (s, 6H), 7.250 (s, 2H), 7.546-7.522 (d, 2H, 7.3 Hz), 7.497-7.475 (d, 4H, 6.6 Hz), 7.403 (s, 4H); ^{13}C NMR (300 MHz, DMSO- d_6): δ 153.162, 145.464, 137.708, 136.933, 135.104, 131.198, 129.599, 128.727, 128.526, 128.181, 127.071, 126.506, 125.864; ESI-MS (acetone) $[M+1]$: 387.4

4.4 Pharmacological evaluation

4.4.1 *In vitro* lipid peroxidation (LPO) assay

4.4.1.1 Materials

All chemicals and solvents used were obtained from commercial sources. The test solutions were centrifuged using Remi centrifuge (R-4C DX). Absorbances were recorded on Thermoscientific UV visible spectrophotometer (Thermosci. Evolution 300).

4.4.1.2 Procedure

The malondialdehyde content; a measure of lipid peroxidation, was assayed in the form of thiobarbituric acid-reactive substances by the method of Wills. Briefly, 0.2 ml brain tissue homogenate, 0.1 ml test sample at five different concentrations, 0.2 ml of 8.1% sodium dodecyl sulfate, 1.5 ml of 20% acetic acid and 1.5 ml of 8% 2-Thiobarbituric acid (TBA) were taken together and final volume of the mixture was adjusted to 4 ml with distilled water and then heated at 95°C for 60 minutes. Then the tubes were cooled to room temperature and final volume was made to 5 ml in each tube using distilled water. 5 ml of butanol: pyridine (15:1) mixture was added to extract the contents and was centrifuged at 4000rpm for 10 minutes. After centrifugation, the upper organic layer was collected and its absorbance was recorded at 532 nm

against an appropriate blank. The above mentioned procedure was followed in duplicate for ascorbic acid (reference standard) and all the test analogues.³⁵

Percentage inhibition of TBA reacting substances (TBARS) formation was calculated with respect to control. The inhibition of lipid peroxidation was determined by calculating the percent (%) decrease in the formation of TBARS.

$$\text{Percentage inhibition} = (\text{Abs}_{\text{control}} - \text{Abs}_{\text{sample}}) \times 100 / \text{Abs}_{\text{control}}$$

4.4.2 Acute toxicity studies

4.4.2.1. Animals

Swiss albino mice weighing 20-25 g of both male and female sex were procured (Bombay Veterinary College, Mumbai) for this study. The animals were housed in group of six in clean plastic cages and maintained under standard laboratory conditions with temperature (22±2) °C, relative humidity (60±10)%, natural light and dark (12:12 hour) cycle with free access to food and water. Animals were acclimatized to laboratory conditions for 15 days before the test. The experimental protocols were approved by the Institutional Animal Ethics Committee (Protocol number: KMKCP/IAEC/161710).

4.4.2.2 Method

Acute toxicity studies were performed on 6 albino mice (3 males+3 females per group) at initial dose of 900 mg/kg p.o. and subsequently thereafter with 800 mg/kg p.o. to study morbidity and mortality, if any, as per OECD-423 guidelines. The test substance was formulated as suspension in an aqueous vehicle using 1% w/v of sodium carboxymethylcellulose as suspending agent. The mice were critically observed for clinical signs, gross behavioral changes and mortality; if any, following administration of the test formulation at different time intervals

like 15 minutes, 30 minutes, 1hr, 2hr, 4hr, 24hr, 48hr and 72hr up to a period of 14 days. The non-lethal dose was determined after acute toxicity studies.

4.4.3 Memory model studies

4.4.3.1 Materials

Piracetam (Standard) was procured as gift sample from Abbott Healthcare Pvt. Ltd., Mumbai and Scopolamine HBr (Toxicant) from Cipla Pvt. Ltd. All other reagents were of highest grades available. Data of memory model studies was analyzed by one way ANOVA using GraphPad Prism 7 software.

4.4.3.2 Groups

Swiss Albino mice were divided into 6 groups each of 6 animals (3 males+3 females per group) for both the model study viz:

Group I: Control group (untreated)

Group II: Toxicant group (Scopolamine 0.4 mg/kg, i.p.)

Group III: Standard treatment group (Piracetam 200mg/kg, p.o.)

Group IV: Test sample A (analogue **20**) at dose level one (50 mg/kg, p.o.)

Group V: Test sample A (analogue **20**) at dose level two (100 mg/kg, p.o.)

Group VI: Test sample B (analogue **13**) at dose level one (50 mg/kg, p.o.)

4.4.3.3 Elevated Plus Maze (EPM) model

EPM model consists of two open arms (25 cm×5 cm) and two closed arms (25 cm×5 cm) extended from a central platform, and the maze was elevated to a height of 25 cm from the floor.

Animals in all groups were subjected to five trials of 5 minutes on the EPM model to establish transfer latency (TL). Then, all animals except toxicant group were administered vehicle/standard/test drug for eight days. On the 8th day, toxicant (Scopolamine HBr) was administered an hour after the administration of last dose to all groups except vehicle control. The animals were exposed to training session after 45min of scopolamine administration. In training session each mice was placed at the end of an open arm, facing away from central platform and time taken by the animal to move from open arm into one of the covered arms with all its four legs was recorded in terms of TL.³⁹

4.4.3.4 Step down inhibitory avoidance test

After EPM, animals were subjected to the step down inhibitory avoidance model study and step down latency (SDL) was determined using Cook's pole apparatus. The animals were trained using a 5 X 5 X 5 cm plywood plank and a floor consisting of 1 mm bronze bars. The left end of the grid was covered with 10 cm high, 7 cm wide and 1.7 cm long wood platform. The mice was placed on the platform with its all four limbs on the platform and allowed to step down. 24 hours later the animals were gently held by the body and lowered on the platform and a timer was activated to measure the latency to step down (i.e. placing all four paws on the grid) and on stepping down it received intermittent foot shock (1 mA) through the grid floor of 5 sec duration until the animal climbed back on the platform. The mice were given three trials until the latency of step down had stabilized. In the test session, on 8th day of treatment after subjecting the animal to toxicant the test was repeated to record SDL to assess retention of memory of learned task. Retention of memory for each animal was calculated in seconds.³⁹

4.4.4 *In vitro* cholinesterase inhibition

4.4.4.1 *Materials*

Acetylthiocholine iodide, acetylcholinesterase from electric eel (AChE), 5,5-dithiobis[2-nitrobenzoic acid] (DTNB), butyrylcholinesterase from equine serum (BuChE), S-butrylthiocholine chloride were purchased from Sigma Chemicals (St. Louis, MO, USA). Galantamine hydrobromide and donepezil were purchased from Tocris Biosciences (Bristol, U.K.) and Cayman Chemical Company (Ann Arbor, MI, USA) respectively. All the other reagents used were of analytical grade. Absorbances were measured using Tecan Infinite M200 microplate reader (Tecan, Switzerland).

4.4.4.2 *Method*

Cholinesterase inhibitory activity of the test samples was determined by Ellman's microplate assay with modification.^{40, 41} For AChE inhibitory assay, 140 μ L of 0.1 M sodium phosphate buffer (pH 8) was first added to each well of a 96-well microplate followed by 20 μ L of the test sample in DMSO and 20 μ L of 0.1 unit/mL AChE. Stock solution for all the samples was prepared at 10 mM in DMSO. The concentration of DMSO in final reaction mixture was maintained at 1%, at which it has no effect on cholinesterase activity. After 15 minutes pre-incubation at room temperature, 10 μ L of 10 mM DTNB was added into each well followed by 10 μ L of 14 mM of acetylthiocholine iodide. Absorbance of the coloured end product was measured at 412 nm for 45 minutes after initiation of enzymatic reaction. For BuChE inhibitory assay, the same procedure as described above was followed except for the use of enzyme and substrate, which were BuChE and S-butrylthiocholine chloride, respectively. Absorbance of the test samples was corrected by subtracting the absorbance of their respective blank (test samples

in DMSO with substrate and DTNB, but without enzyme). A set of six concentrations was used to estimate the 50% inhibitory concentration (IC_{50}). Each test was conducted in quadruplicate and repeated at least twice.

Funding

This research did not receive any specific grant from funding agencies in the public, commercial, or not-for-profit sectors.

References

1. Sheikh, S.; Safia; Haque, E.; Mir, S. S. Neurodegenerative Diseases: Multifactorial Conformational Diseases and Their Therapeutic Interventions. *J. Neurodegener. Dis.* **2013**, 20 (13), 1–8.
2. Anand, R.; Gill, K. D.; Mahdi, A. A. Therapeutics of Alzheimer's disease: Past, present and future. *Neuropharmacology* **2014**, 27–50.
3. Selkoe, D. J. Alzheimer's Disease Is a Synaptic Failure. *Science* **2002**, 298 (5594), 789–791
4. Bateman, R. Alzheimer's disease and other dementias: Advances in 2014. *The Lancet Neurology* **2015**, 4–6.
5. Tripathi, A.; Srivastava, U. C. Acetylcholinesterase: A Versatile Enzyme of Nervous System. *Ann. Neurosci.* **2010**, 15 (4), 106–111.
6. Li, Q.; Yang, H.; Chen, Y.; Sun, H. Recent progress in the identification of selective butyrylcholinesterase inhibitors for Alzheimer's disease. *Eur. J. of Med. Chem.* **2017**, 132, 294–309.
7. Giacobini, E. Do cholinesterase inhibitors have disease-modifying effects in Alzheimer's disease? *CNS Drugs* **2001**, 15 (2), 85–91.

8. Bartus, R. T.; Dean, R. L.; Beer, B.; Lippa, Cholinergic Drugs and Human Cognitive Performance. *A. S. Science* **1982**, *217*, 393-424.
9. Davis, K. L.; Powchik, P. Tacrine. *Lancet* **1995**, *345* (8950), 625-630.
10. Dvir, H.; Silman, I.; Harel, M.; Rosenberry, T. L.; Sussman, J. L. Acetylcholinesterase: From 3D structure to function. *Chemico-Biological Interactions* **2010**, *187*, 10–22.
11. Bourne, Y.; Taylor, Z. R., Marchot, P. Structural insights into ligand interactions at the acetylcholinesterase peripheral anionic site. *The EMBO Journal* **2003**, *22*, 1–12.
12. Kryger, G.; Silman, I.; Sussman, J. L.; Structure of acetylcholinesterase complexed with E2020 (Aricept®): Implications for the design of new anti-Alzheimer drugs. *Structure* **1999**, *7*, 297–307.
13. Alvarez, A.; Opazo, C.; Alarcón, R.; Garrido, J.; Inestrosa, N. C. Acetylcholinesterase promotes the aggregation of amyloid- β -peptide fragments by forming a complex with the growing fibrils. *Journal of Molecular Biology* **1997**, *272*, 348–361.
14. Bartolini, M.; Bertucci, C.; Cavrini, V.; Andrisano, V. β -Amyloid aggregation induced by human acetylcholinesterase: Inhibition studies. *Biochemical Pharmacology* **2003**, *65*, 407–416.
15. Inestrosa, N. C.; Dinamarca, M. C.; Alvarez, A. Amyloid-cholinesterase interactions. *FEBS Journal* **2003**, *275*, 625–632.
16. Singla, S.; Piplani, P. Coumarin derivatives as potential inhibitors of acetylcholinesterase: Synthesis, molecular docking and biological studies. *Bioorg & Med. Chem.* **2016**, *24* (19), 4587-99.
17. Yoon, Y. K.; Ali, M. A.; Wei, A.C.; Choon, T. S.; Khaw, K. Y.; Murugaiyah, V.; Osman, H.; Masand, V. H. Synthesis, characterization, and molecular docking analysis of novel benzimidazole derivatives as cholinesterase inhibitors. *Bioorg Chem.* **2013**, *49*, 33-39.

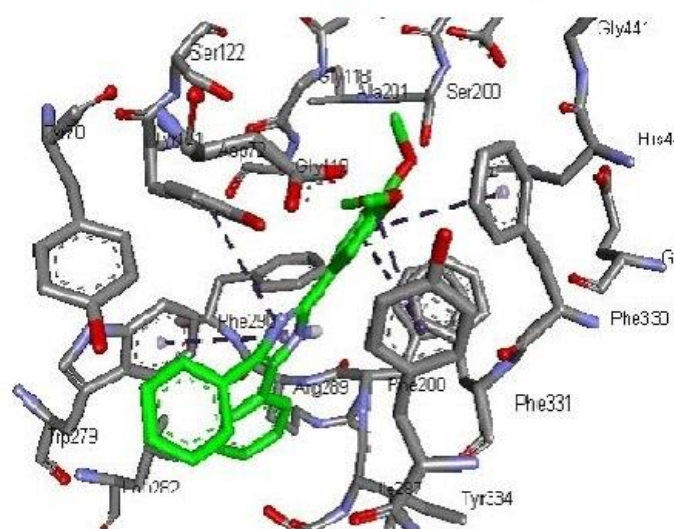
18. Brahmacharia, G.; Choob, C.; Ambured, P.; Roy, K. *In vitro* evaluation and *in silico* screening of synthetic acetylcholinesterase inhibitors bearing functionalized piperidinepharmacophores. *Bioorg& Med. Chem.* **2015**, *23* (13), 27-34.
19. Shalini, K.; Sharma, P. K.; Kumar, N. Imidazole and its biological activities: A review, *Der Chemica Sinica* **2010**, *1* (3), 36-47.
20. Maryamabadi, A.; Hasaninejad, A.; Nowrouzi, N.; Mohebbi, G. Green synthesis of novel spiro-indenoquinoxaline derivatives and their cholinesterases inhibition activity. *Bioorg& Med. Chem.* **2017**, *25* (7), 2057-2064.
21. Maryamabadi, A.; Hasaninejad, A.; Nowrouzi, N.; Mohebbi, G. Application of PEG-400 as a green biodegradable polymeric medium for the catalyst-free synthesis of spiro-dihydropyridines and their use as acetyl and butyrylcholinesterase inhibitors. *Bioorg& Med. Chem.* **2016**, *24* (6), 1408–1417
22. Rahim, F.; Javed, M. T.; Ullah, H.; Wadood, A.; Taha, M.; Ashraf, M.; Qurat-Ul-Ain; Khan, M. A.; Khan, F.; Mirza, S. Synthesis, molecular docking, acetylcholinesterase and butyrylcholinesterase inhibitory potential of thiazole analogs as new inhibitors for Alzheimer disease. *Bioorg. Chem.* **2015**, *62*, 106–116.
23. Morris, G. M.; Lim-Wilby, M. Molecular docking. *Methods Mol. Biol.* **2008**, *443*, 365–382.
24. Verdonk, M. L.; Cole, J. C.; Hartshorn, M. J.; Murray, C. W.; Taylor, R. D. Improved protein-ligand docking using GOLD. *Proteins Struct.Funct.Genet.* **2003**, *52* (4), 609–623.
25. Jackisch, R.; Forster, S.; Kammerer, M.; Rothmaier, A. K.; Ehret, A.; Zentner, J.; Feuerstein, T. J. Inhibitory potency of choline esterase inhibitors on acetylcholine release and choline esterase activity in fresh specimens of human and rat neocortex. *J Alzheimers Dis.* **2009**, *16* (3), 635-647.

26. Howes, M. J.; Houghton, P. J. Acetylcholinesterase inhibitors of natural origin. *Int. J. of Biomed. & Pharm. Sci.* **2009**, *1*, 67-86.
27. Chen, Y.; Xu, X.; Fu, T.; Li, W.; Liu, Z.; Sun, H. Discovery of New Scaffolds from Approved Drugs as Acetylcholinesterase Inhibitors. *RSC Adv.* **2015**, 1-8.
28. Meng, F. C.; Mao, F.; Shan, W. J.; Qin, F.; Huang, L.; Li X. S. Design, synthesis, and evaluation of indanone derivatives as acetylcholinesterase inhibitors and metal-chelating agents. *Bioorg & Med. Chem. Letters* **2012**, *22* (13), 4462-4466.
29. Martis, E. A. F.; Chandarana, R. C.; Shaikh, M. S.; Ambre, P. K.; D'Souza, J. S.; Iyer, K. R.; Coutinho, E. C.; Nandan, S. R.; Pissurlenkar, R. R. S. Quantifying Ligand-Receptor Interactions for Gorge Spanning Acetylcholinesterase Inhibitors for the Treatment of Alzheimer's disease. *J. Biomol. Struct. Dyn.* **2014**, 1-69.
30. Imberty, A.; Hardman, K. D.; Carver, J.P.; Perez, S. Molecular modelling of protein-carbohydrate interactions: Understanding the specificities of two legume lectins towards oligosaccharides. *Glycobiology*, **1991**, *1*, 631-642.
31. Gleeson, M. P.; Hersey, A.; Hannongbua, S. *In-Silico* ADME Models: A General Assessment of their Utility in Drug Discovery Applications. *Curr.Top. Med. Chem.* **2011**, *11*, 358-381.
32. DunnIII, W. J.; Koehler, M. G.; Grigoras, S. The role of solvent-accessible surface area in determining partition coefficient. *J.of Med. Chem.* **1987**, *30*, 1121-1126.
33. Suite, Small-Molecule Drug Discovery 2013: QikProp, version 3.3, User Manual, Schrödinger,, LLC, New York, NY**2013**.

34. Sangshetti, J. N.; Kokare, N. D.; Kotharkara, S. A.; Shinde, D. B. Ceric Ammonium nitrate catalysed three component one-pot efficient synthesis of 2,4,5-triphenyl-1H-imidazoles. *J. Chem. Sci.* **2008**, *120* (5), 463-467.
35. Garcia, Y. J.; Rodriguez-Malaver, A. J.; Penaloza, N. Lipid peroxidation measurement by thiobarbituric acid assay in rat cerebellar slices. *J. Neurosci. Methods* **2005**, *144* (1), 127-135.
36. Alam, M. N.; Bristi, N. J.; Rafiquzzaman, M. Review on *in vivo* and *in vitro* methods evaluation of antioxidant activity. *Saudi Pharm. J.* **2013**, *21* (2), 143-152.
37. Sybyl version 8.1.1, Tripos International, St. Louis, Missouri, Portugal.
38. GOLD version 5.2.2, CCDC Ltd., UK.
39. Bryan, K. J.; Lee, H.; Perry, G.; Smith, M. A.; Casadesus, G. Transgenic Mouse Models of Alzheimer's Disease: Behavioral Testing and Considerations. *Methods Behav. Anal. Neurosci.* **2009**, 1-10.
40. Ellman, G. L.; Courtney, K. D.; Andres, V.; Featherstone, R. M. A new and rapid colorimetric determination of acetylcholinesterase activities. *Biochem. Pharmacol.* **1961**, *7*, 88-95.
41. Yeong, K. Y.; Liew, W. L.; Murugaiyah, V.; Ang, C. W.; Osman, H.; Tan, S. C. Ethyl nitrobenzoate: a novel scaffold for cholinesterase inhibition. *Bioorg. Chem.*, **2017**, *70*, 27-33.

Highlights

- Docking studies of 2-substituted-4,5-diphenyl-1H-imidazoles in AChE active site.
- Based on Docking and *in silico* ADME results, synthesis of some analogues.
- Study neuroprotective role, toxicity and effect of analogues on memory in animals.
- Detailed mechanistic *in vitro* AChE and BuChE inhibition studies.



Analogue within AChE active site

